Int. J. Solids Structures, 1974, Vol. 10, pp. 853–862. Pergamon Press. Printed in Gt. Britain.

PLASTIC DEFORMATION AND LATENT STRAIN ENERGY IN A POLYCRYSTALLINE ALUMINUM MODEL

K. S. HAVNER and C. SINGH

Department of Civil Engineering, North Carolina State University, Raleigh, North Carolina 27607, U.S.A.

and

R. VARADARAJAN

Delon Hampton & Associates, Washington, D.C., U.S.A.

(*Received* 23 *August* 1973)

Abstract—A crystalline aggregate model of aluminum is evaluated for nearly uniaxial stressing. Progression of crystallographic slip, a hysteresis effect in a strain cycle, and heat generated and latent strain energy stored during plastic deformation are investigated. Close correspondence is found between calculated and experimental results for percentages of heat and latent energy. A proof is included that total mechanical energy dissipated is absolutely less than macroscopic plastic work for all paths.

1. INTRODUCTION

The evolution of theoretical polycrystalline plasticity (or the "physical" theory of plasticity) from its beginnings in Taylor's famous model and principle of minimum shears[1, 2] to 1970 is well-summarized by Lin[3] and Hutchinson[4]. Subsequent to these reviews a model has been developed and presented by Havner[5] which is comparable to but distinctly different from the self-consistent models of Lin and Hershey–Hill[6, 7] studied in [3 and 4]. This model has been analytically confirmed as a rational discretization in [8] and extended to include finite deformation effects in [9]. An initial quantitative study of the model by Havner and Varadarajan[10] focuses upon determination of subsequent yield surfaces for aluminum and numerical confirmation of basic macroscopic inequalities of the general theory developed by Hill[11].

In the present paper we further investigate theoretical response of the aluminum aggregate model described in [10]. Aspects of behavior studied include (a) progression of crystallographic slip with (nearly) uniaxial stressing well into the plastic range, (b) computation of a narrow hysteresis loop in an unloading–reloading cycle, and (c) determination of the heat and latent strain energy which accompany macroscopic deformation.

2. REVIEW OF THE BASIC THEORY AND MODEL

The following is taken from [10]. At the outset we define a microscopic continuum point-of-view wherein a crystal material "point" has dimensions of order 10^{-3} mm (i.e. $> 10^3$ lattice spacings). This is consistent with the minimum level at which a continuum mechanics description of plastic deformation in metals can be judged physically meaningful (see, for

example, pertinent discussions in [9, 12, 13]). The mechanical behavior is taken to be representable via two *kinematically* independent mechanisms of deformation (which are phenomenological averages of complex processes occurring within the lattice volume defined by the "point"). These mechanisms are: (a) elastic (mechanically recoverable) infinitesimal strain of the lattice, and (b) simple glide, on well-defined crystallographic slip systems, which translates material "lines" of points (i.e. glide packets) relative to one another but leaves the (averaged) crystal structure unchanged.

Restricting the analysis to small strains, the local constitutive and field equations in terms of increments are

$$\delta\boldsymbol{\varepsilon} = \mathscr{D}^T \delta\mathbf{u} = \mathbf{C}\,\delta\boldsymbol{\sigma} + \mathbf{N}^T \delta\gamma, \tag{1}$$

$$\delta\tau_{cr} = \mathbf{H}(\gamma)\,\delta\gamma, \tag{2}$$

and $\mathscr{D}\,\delta\boldsymbol{\sigma} = \mathbf{0}$ (neglecting inertia and body forces). For a critical (i.e. potentially active) slip system:

$$\tau_{cr}^k \equiv \tau_0 + \int \delta\tau_{cr}^k = \mathbf{N}_k\,\boldsymbol{\sigma}, \tag{3}$$

$$\delta\tau_{cr}^k \geq \mathbf{N}_k\,\delta\boldsymbol{\sigma}, \qquad \delta\gamma_k \geq 0, \tag{4a,b}$$

$$\delta\gamma_k(\delta\tau_{cr}^k - \mathbf{N}_k\,\delta\boldsymbol{\sigma}) = 0 \qquad \text{(for each } k\text{)}. \tag{5}$$

In these equations $\boldsymbol{\sigma}$ and $\boldsymbol{\varepsilon}$ are vector representations of micro-stress and -strain: $\boldsymbol{\sigma} = (\sigma_{11}, \sigma_{22}, \sigma_{33}, \sqrt{2}\sigma_{23}, \sqrt{2}\sigma_{31}, \sqrt{2}\sigma_{12})$; $\boldsymbol{\varepsilon} = (\varepsilon_{11}, \varepsilon_{22}, \varepsilon_{33}, \sqrt{2}\varepsilon_{23}, \sqrt{2}\varepsilon_{31}, \sqrt{2}\varepsilon_{12})$. The operator $\mathscr{D}$ is a 3 by 6 matrix representation of the spatial gradient; $\mathbf{u}$ is the displacement; $\mathbf{C}$ is the positive-definite crystal elastic compliance matrix referred to the specimen axes; and $\mathbf{N}$ is the N by 6 transformation matrix between these axes and the local crystallographic slip systems, $\mathbf{N}_k$ denoting the kth row vector. The $\delta\gamma$ are incremental plastic shears; τ_{cr}^k is a critical shear stress (crystal shear strength) initially equal to τ_0; and $\mathbf{H}(\gamma)$ is a general crystal hardening matrix[14, 15] considered to be at least positive-semidefinite. Opposite senses of slip in the same crystallographic slip system are denoted by distinct k's so that $\delta\gamma_k$ is always non-negative. (Throughout the paper, juxtaposition of matrix and vector or vector and vector implies inner product multiplication.)

Consider a thin-walled metal tube subjected to, say, axial load and internal pressure. The wall thickness of specimens studied experimentally in combined loading tests is often in the range 1–2 mm, with from 10 to 30 gr through the thickness (see, e.g. [16, 17]). Thus, as an idealization of the physical situation, we assume a thickness of 1 mm and define a unit cube $V = 1$ mm^3 containing on the order 1000 crystal grains in the corresponding "flat sheet" representation (i.e. a *macroscopic* plane stress problem). Further, we wish the mathematical model to correspond to a macroscopically homogeneous physical specimen (that is, one for which strain gage readings over distances of at least 1 mm on the surface are essentially uniform from one location to another). We therefore require all the unit cubes to deform identically and take the longitudinal and transverse faces to be planes of symmetry under biaxial macroscopic straining. (For additional discussion see [5].) Thus, for quasi-static deformation, we adopt as a model for analysis a unit cube (of generally anisotropic crystals) on each of whose faces either (1) a particular incremental displacement component is prescribed, to give the appropriate macroscopic strain increment, or (2) the associated traction is zero.

3. MACROSCOPIC INEQUALITIES

As shown in [5], the model of identically deforming unit cubes satisfies the averaging theorem

$$\overline{\boldsymbol{\sigma}\boldsymbol{\varepsilon}} = \bar{\boldsymbol{\sigma}}\bar{\boldsymbol{\varepsilon}} \tag{6}$$

wherein $\boldsymbol{\sigma}(\mathbf{x})$, $\boldsymbol{\varepsilon}(\mathbf{x})$ are statically admissible stress and kinematically admissible strain fields respectively and a bar above a vector or scalar field denotes the aggregate volume average. Corresponding operational definitions of macroscopic stress and strain are

$$\boldsymbol{\sigma}_M = \bar{\boldsymbol{\sigma}}, \qquad \boldsymbol{\varepsilon}_M = \bar{\boldsymbol{\varepsilon}}. \tag{7a,b}$$

Equation (6) also is satisfied by boundary conditions on a representative macroelement of either uniform loading or uniform constraint[11, 18] and was first established by Bishop and Hill[19] based upon a "non-correlation" hypothesis. These various postulates on boundary data are equally viable and for purposes of theoretical studies (6) may be considered a minimal prescription of macroscopically uniform fields.

Let $\mathbf{L}_M$ denote the macroscopic matrix of elastic moduli of the aggregate cube and $\mathbf{L}_c$ denote the elastic moduli of the individual crystals referred to the lattice axes. There follows[5, 10]

$$\mathbf{L} = \mathbf{A}^T\mathbf{L}_c\mathbf{A}, \qquad \mathbf{L}_M = \overline{\boldsymbol{\Psi}^T\mathbf{L}\boldsymbol{\Psi}}, \tag{8a,b}$$

in which $\mathbf{A}$ is the stress (strain) vector orthogonal transformation matrix, determined by the grain orientation relative to the specimen (cube) axes, and $\boldsymbol{\Psi}(\mathbf{x})$ is a dimensionless tensor (matrix) function of position due to the elastic heterogeneity (i.e. $\delta\boldsymbol{\varepsilon}^{(e)} = \boldsymbol{\Psi}\,\delta\boldsymbol{\varepsilon}_M$ in assumed elastic response). We also denote $\mathbf{C}_M = \mathbf{L}_M^{-1}$ (macroscopic elastic compliance matrix) and define incremental macroscopic plastic strain and plastic stress (or negative "slip stress") operationally as[5]

$$\delta\boldsymbol{\varepsilon}_M^p = \delta\boldsymbol{\varepsilon}_M - \mathbf{C}_M\,\delta\boldsymbol{\sigma}_M, \tag{9a}$$

$$\delta\boldsymbol{\sigma}_M^p = \mathbf{L}_M\,\delta\boldsymbol{\varepsilon}_M - \delta\boldsymbol{\sigma}_M. \tag{9b}$$

The following fundamental macroscopic inequalities are then satisfied[10,11,20],

$$\delta\boldsymbol{\sigma}_M\,\delta\boldsymbol{\varepsilon}_M^p > 0, \qquad \delta\boldsymbol{\sigma}_M^*\,\delta\boldsymbol{\varepsilon}_M^p \le 0, \tag{10a,b}$$

$$\delta\boldsymbol{\varepsilon}_M\,\delta\boldsymbol{\sigma}_M^p > 0, \qquad \delta\boldsymbol{\varepsilon}_M^*\,\delta\boldsymbol{\sigma}_M^p \le 0, \tag{11a,b}$$

wherein $\delta\boldsymbol{\sigma}_M^*$, $\delta\boldsymbol{\varepsilon}_M^*$ are any associated macroscopic pair corresponding to purely elastic response of the aggregate. These inequalities have been demonstrated on a number of subsequent yield surfaces for the aluminum aggregate model in [10]. The first pair (10a,b) are of course the basic stability and generalized normality postulates of the mathematical theory of (infinitesimal) plasticity[21–23]; the second pair are their dual.

4. WORK AND ENERGY

We now consider macroscopic and internal measures of work and energy pertinent to the numerical studies reported in Section 6. For completeness we present independent derivations of some relationships also to be found in [20].

The obvious operational definitions of macroscopic (apparent) elastic work and (apparent) plastic work per unit volume are

$$W_E = \tfrac{1}{2}\boldsymbol{\sigma}_M\,\mathbf{C}_M\,\boldsymbol{\sigma}_M, \qquad W_P = \int \boldsymbol{\sigma}_M\,\mathrm{d}\boldsymbol{\varepsilon}_M^p \tag{12a,b}$$

whereas internal strain energy is defined as

$$U = \tfrac{1}{2}\overline{\boldsymbol{\sigma}\mathbf{C}\boldsymbol{\sigma}} \tag{13}$$

with $\mathbf{C} = \mathbf{A}^T\mathbf{C}_c\mathbf{A}$. ($\mathbf{C}_c = \mathbf{L}_c^{-1}$ is the crystal elastic compliance matrix referred to the lattice axes.) Similarly, internal plastic work (mechanical energy dissipated as heat) is defined

$$Q = \int \overline{\tau_{cr}\, \mathrm{d}\gamma} = \int \overline{\boldsymbol{\sigma}\, \mathrm{d}\boldsymbol{\varepsilon}^p} \tag{14}$$

with $\mathrm{d}\boldsymbol{\varepsilon}^p = \mathbf{N}^T\, \mathrm{d}\boldsymbol{\gamma}$ from (1). The total mechanical work done on the aggregate cube is equivalently expressed (from (6))

$$W = \int \boldsymbol{\sigma}_M\, \mathrm{d}\boldsymbol{\varepsilon}_M = \int \overline{\boldsymbol{\sigma}\, \mathrm{d}\boldsymbol{\varepsilon}}. \tag{15}$$

Thus, from (1), (9a) and (12–15),

$$W_E + W_P = W = U + Q. \tag{16}$$

We wish to prove that $U > W_E$, hence $W_P > Q$.

Let $\boldsymbol{\sigma}^r = \boldsymbol{\sigma} - \boldsymbol{\sigma}^{(e)}$ denote the residual microstress field that would remain if the specimen could be elastically unloaded to zero macrostress, with $\boldsymbol{\sigma}^{(e)}$ given as [10]

$$\boldsymbol{\sigma}^{(e)} = \mathbf{L}\boldsymbol{\Psi}\mathbf{C}_M\boldsymbol{\sigma}_M. \tag{17}$$

W_E can then be expressed (from (8b) and (17))

$$W_E = \overline{\tfrac{1}{2}\boldsymbol{\sigma}^{(e)}\mathbf{C}\boldsymbol{\sigma}^{(e)}} \equiv \tfrac{1}{2}\overline{(\boldsymbol{\sigma} - \boldsymbol{\sigma}^r)\mathbf{C}(\boldsymbol{\sigma} - \boldsymbol{\sigma}^r)}. \tag{18}$$

Thus, with the aid of (6), since $\boldsymbol{\sigma}^r$ is statically admissible at $\boldsymbol{\sigma}_M = 0$ whereas $\mathbf{C}\boldsymbol{\sigma}^{(e)} = \boldsymbol{\Psi}\mathbf{C}_M\boldsymbol{\sigma}_M$ is kinematically admissible for arbitrary $\boldsymbol{\sigma}_M$[5, 10],

$$W_E = U - U_R \tag{19}$$

with

$$U_R = \tfrac{1}{2}\overline{\boldsymbol{\sigma}^r\mathbf{C}\boldsymbol{\sigma}^r}, \tag{20}$$

the residual or latent strain energy. There follows from (16)

$$W_P - Q = U - W_E = U_R > 0. \qquad \text{(Q.E.D.)} \tag{21}$$

We conclude that the total mechanical energy dissipated in heat is absolutely less than the (apparent) macroscopic plastic work for all paths. This of course does not imply that $\delta W_P > \delta Q$ in all steps. Indeed, although we may require $\delta Q = \overline{\tau_{cr}\, \delta\gamma} > 0$, it may easily happen that $\delta W_P = \boldsymbol{\sigma}_M\, \delta\boldsymbol{\varepsilon}_M^p < 0$ as is well-known experimentally. (Also see discussions in [11 and 20].)

5. SOLUTION OF THE DISCRETE MODEL

The discretization of the aggregate model and the general solution for crystal shears in terms of overall matrix equations is fully described in [5]. Herein we briefly present principal features of the numerical analysis without introducing the aggregate matrix symbolism (for which the reader is referred to [5], [8] or [10]).

By simple substitutions (1–5) can be recast as the set of field equations

$$\mathscr{D}\{\mathbf{L}(\mathscr{D}^T\, \delta\mathbf{u} - \mathbf{N}_j^T\, \delta\gamma_j)\} = \mathbf{0} \tag{22}$$

and the linear complementarity problem on critical systems (see [9])

$$(h_{kj} + \mathbf{N}_k \mathbf{L} \mathbf{N}_j^T)\, \delta\gamma_j - \mathbf{N}_k \mathbf{L} \mathscr{D}^T\, \delta\mathbf{u} = \delta\lambda_k, \tag{23}$$

$$\delta\lambda_k \geq 0, \qquad \delta\gamma_k \geq 0, \qquad \delta\gamma_k\, \delta\lambda_k = 0 \tag{24a–c}$$

(wherein the h_{kj} are the elements of $\mathbf{H}$). The external boundary conditions correspond to an increment of prescribed macrostrain $\delta\boldsymbol{\varepsilon}_M$ and appropriate zero tractions, as more fully explained in the next section (also see [10]). The field equations are discretized, in effect, by subdividing the aggregate into tetrahedral elements, henceforth referred to as crystallites, and introducing the simplest *convergent* approximation[8] of linearly varying displacement fields and spatially uniform plastic shears within each crystallite. The discrete counterpart of (22) is readily solved to obtain (in combination with (1))

$$\delta\sigma_{(q)} = (\mathbf{L}\boldsymbol{\psi})_{(q)}\, \delta\boldsymbol{\varepsilon}_M - \overline{\mathbf{Z}(q, q')(\mathbf{N}_j^T\, \delta\gamma_j)_{(q')}} \tag{25}$$

in which q, q' denote crystallites and $\boldsymbol{\psi}_{(q)}$ and the discrete influence function $\mathbf{Z}(q, q')$ are determined from the inverse of the aggregate elastic "stiffness" matrix[5] and the local moduli $\mathbf{L}_{(q)}$.

Upon substituting (25) and (1) into (23, 24) we find that the linear complementarity problem can be alternatively posed as either of the quadratic programming problems[5]

$$\left.\begin{aligned} &\text{minimize} \quad \tfrac{1}{2}\, \overline{\delta\gamma_k(h_{kj} + p_{kj})\, \delta\gamma_j} - \overline{\delta\gamma_k\, \delta f_k} \\ &\text{subject to} \quad \delta\gamma_k \geq 0, \end{aligned}\right\} \tag{26}$$

or [9]

$$\left.\begin{aligned} &\text{maximize} \quad -\overline{\delta\gamma_k(h_{kj} + p_{kj})\, \delta\gamma_j} \\ &\text{subject to} \quad (h_{kj} + p_{kj})\, \delta\gamma_j - \delta f_k \geq 0, \end{aligned}\right\} \tag{27}$$

with k, j ranging only over critical systems and

$$p_{kj}(q, q') = \mathbf{N}_k(q)\mathbf{Z}(q, q')\mathbf{N}_j^T(q'), \tag{28}$$

$$\delta f_k(q) = (\mathbf{N}_k \mathbf{L}\boldsymbol{\psi})_{(q)}\, \delta\boldsymbol{\varepsilon}_M. \tag{29}$$

Here, as in [10], (26) is chosen with the method of Hildreth and D'Esopo[24] adopted for solution.

6. NUMERICAL STUDIES

Because of extensive computer time and large storage requirements the actual model calculated is limited to approx 400 gr (crystallites) within the unit cube (Fig. 1). Every crystallite has twelve crystallographically equivalent slip systems $\{111\}\langle 1\bar{1}0\rangle$, or twenty-four counting opposite senses of slip as distinct systems for a total of 2304 in each quadrant. The faces $x_3 = \pm 1/2$ are free and macroscopic biaxial strains $\bar{\varepsilon}_1$, $\bar{\varepsilon}_2$ are imposed by specifying uniform normal displacements on the faces x_1, $x_2 = 1/2$ (choosing the origin at the cube centroid) with tangential tractions set equal to zero. We take x_1, $x_2 = 0$ to be planes of symmetry, hence normal displacements are zero on these interior faces of the quadrant.

The symmetric crystal elastic compliance $\mathbf{C}_c$ for aluminum, in units of 10^{-3} mm^2/kg (as converted from [25]), has elements $(C_c)_{11} = (C_c)_{22} = (C_c)_{33} = 0{\cdot}1559$, $(C_c)_{12} = (C_c)_{13} =$

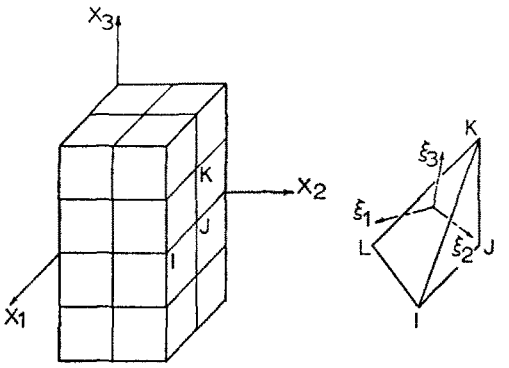

Fig. 1. One quadrant of unit cube and a typical tetrahedral crystallite.

$(C_c)_{23} = -0{\cdot}0569$, and $(C_c)_{44} = (C_c)_{55} = (C_c)_{66} = 0{\cdot}1726$, with all other nonsymmetric elements zero. The distribution of grain orientations is chosen so as to simulate a statistically isotropic specimen. From the aggregate elastic solution the isotropic properties are determined approximately as $E = 10{\cdot}15 \times 10^6$ psi, $G = 3{\cdot}74 \times 10^6$ psi, and $\nu = 0{\cdot}354$[10]. Lastly, Taylor hardening[1, 26] is adopted with a constant hardening modulus $h = 7{\cdot}5$ kg/mm^2 (i.e. $h_{kj} = h$ for k, j in the same crystallite and zero otherwise). For further discussion of the computational problem see [10].

The present studies are related to a biaxial strain path which roughly corresponds to uniaxial stressing. In the elastic range the correspondence is made precise by choosing the ratio $\delta\bar{\varepsilon}_1 : \delta\bar{\varepsilon}_2 = 2{\cdot}85 : -1$ as determined from the aggregate moduli. These are calculated from (8b) (for the macroscopic plane stress state) to be $(L_M)_{11} = 8060$, $(L_M)_{12} = (L_M)_{21} = 2895$ and $(L_M)_{22} = 8247$ kg/mm^2. The resulting stress–strain plots are displayed in Fig. 2

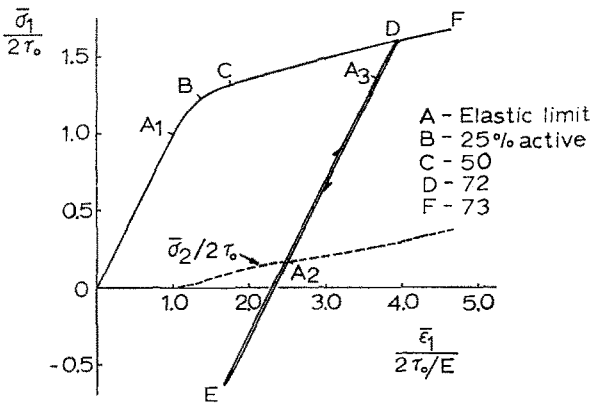

Fig. 2. Aggregate stress–strain curves and percentages of active slip systems.

in terms of the indicated dimensionless variables (which presentation is independent of the choice of τ_0 as explained in [10]).

Consider first that portion of the curve for $\bar{\sigma}_1/2\tau_0$ from the origin to point D. (The prescribed strain path is changed from $2{\cdot}85 : -1$ to $2 : -1$ at $\bar{\varepsilon}_1/(2\tau_0/E) = 1{\cdot}310$, just before point B.) The maximum number of slip systems that one expects could become active with

increasing plastic deformation (as elastic increments become negligible) is, on average, 5 per gr[1, 27]. We therefore assume 480 out of 1152 crystallographic systems to be the total number of *simultaneously active* systems possible within a quadrant of the unit cube. Correspondingly, we can relate the progression of crystallographic slip to continued plastic straining via the percentage of active to potentially active systems at each stage. Thus, at point A, the initial elastic limit, a single slip system is engaged. (There is no discernible yielding, however, until a number of additional systems have been activated.) Points B and C mark stages at which 25 and 50 per cent respectively of possible systems are active, and 72 per cent (344 systems per quadrant) are active at D. It may be noted that the tangent modulus of the curve is very nearly constant after about two thirds of the total potential systems have been activated.

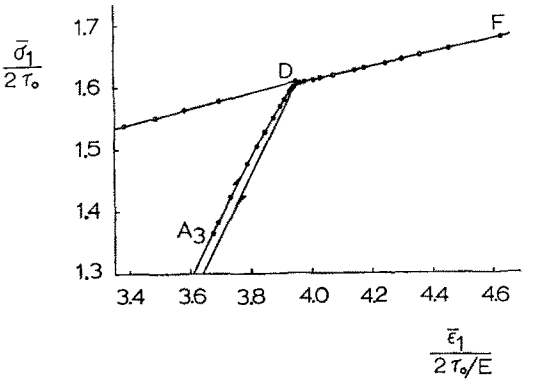

Fig. 3. Stress–strain curve in the vicinity of point D.

At point D the aggregate model is unloaded by following the reversed strain path $\delta\bar{\varepsilon}_1 : \delta\bar{\varepsilon}_2 = -2{\cdot}85 : 1$, such that DA_2 parallels $0A_1$ with $\bar{\sigma}_2$ constant. Point A_2 is the new elastic limit, but "yielding" is remarkably gradual (consistent with generally observed physical behavior) and at point E only 10 per cent of the possible systems are active. These few are enough, however, to produce a narrow-band hysteresis loop as the aggregate is reloaded along $2{\cdot}85 : -1$ with the next elastic limit (once more where a single system is engaged) at point A_3. The plots in the vicinity of D are shown in finer detail in Fig. 3. The yielding is again quite gradual (although more pronounced than along the portion A_2E) until the previous point D is approached. Near that state a large number of potential slip systems are "lying in wait" as it were. Accordingly, the curve begins to bend sharply, passing below D, as the percentage of systems activated in going from $\bar{\varepsilon}_1/(2\tau_0/E) = 3{\cdot}913$–$3{\cdot}980$ rapidly increases from 10 to 63 per cent. The incremental strain path is held constant $(2{\cdot}85 : -1)$ in continuing to point F with the result that the (approximately) constant slope of the curve toward the end differs slightly from that of the segment before D (corresponding to the path $2 : -1$). Seventy-three per cent of possible systems are active at F and 79 per cent of the crystallites have three or more active systems, all the others having two each.

We now turn attention to the computation of work and energy in the aggregate model. For the macroscopic plane stress state and Taylor hardening the equations for W, W_E and Q can be expressed

$$W = \int(\bar{\sigma}_1\,\overline{\mathrm{d}\varepsilon_1} + \bar{\sigma}_2\,\overline{\mathrm{d}\varepsilon_2}), \tag{30}$$

$$W_E = \tfrac{1}{2}(C_{11})_M \bar{\sigma}_1^2 + (C_{12})_M \bar{\sigma}_1 \bar{\sigma}_2 + \tfrac{1}{2}(C_{22})_M \bar{\sigma}_2^2, \tag{31}$$

$$Q = \tau_0 \Sigma \bar{\gamma}_k + \frac{h}{2}(\Sigma \overline{\gamma_k})^2, \tag{32}$$

in which $\Sigma\gamma_k$ denotes summation over the slip systems within a crystallite. The macroscopic compliances are $(C_M)_{11} = 0{\cdot}1420$, $(C_M)_{12} = -0{\cdot}04985$ and $(C_M)_{22} = 0{\cdot}1388 \times 10^{-3}$ mm^2/kg (from the inversion of $\mathbf{L}_M$). W, W_E and Q are computed directly at each stage of the deformation after which W_P and U_R are determined from (16 and 21).

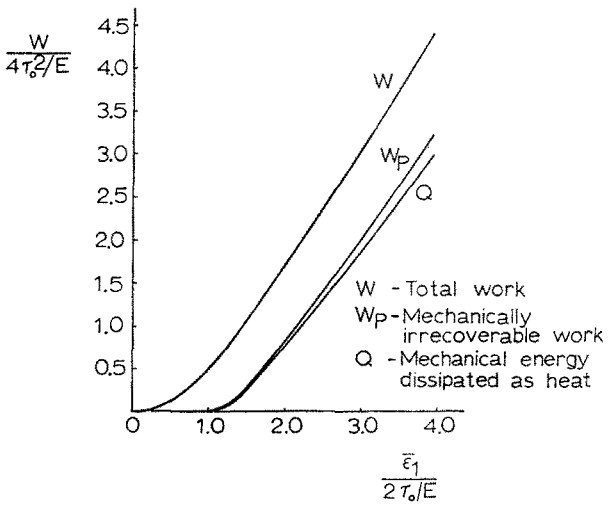

Fig. 4. Work and energy dissipated as heat.

In presenting the results we choose to display only W, W_P and Q since W_E, U_R and U are merely differences between respective pairs of these curves. Non-dimensionalized values (typically, Work/$(4\tau_0^2/E)$ per unit volume) are plotted versus dimensionless strain $\bar{\varepsilon}_1/(2\tau_0/E)$. (Again, this presentation is independent of τ_0.) The calculated curves are shown in Fig. 4 corresponding to portion $0D$ of the stress–strain curve in Fig. 2. Of particular interest is the ratio Q/W_P which can easily be compared with experimentally determined values. From the strain $\bar{\varepsilon}_1/(2\tau_0/E) = 1{\cdot}25$ (at which W_P is 10 per cent of W) onward this ratio averages 93 per cent with a mean deviation of about one-half per cent. Thus, according to the model approximately 7 per cent of the mechanically irrecoverable work W_P is stored as latent strain energy U_R.

The first noteworthy experimental study of the heat generated during plastic deformation is the classic work by Farren and Taylor[28] on extension of steel, copper and aluminum specimens. Subsequent investigations of latent energy in metal rods after large twisting were reported by Taylor and Quinney[29, 30]. In the various experiments on aluminum the measured latent energy averaged about 8 per cent (varying between 6 and 9)[28, 30]. Later studies by Dillon[31] determined the heat generated during cyclic straining of aluminum to be 94 per cent of the macroscopic plastic work, whence 6 per cent was stored as latent strain energy. (All experiments by Taylor and his colleagues were in a range of large deformations whereas Dillon's work was at small strain.) The close correspondence between the various experimental results and the present theory and model is certainly worth remarking. (The

only previous theoretical calculations of which the authors are aware are those by Lin and Ito[32] which are for zinc, of h.c.p. structure, and indicate a quite different trend.)

7. CLOSING REMARKS

Studies of metal polycrystal models as in [3, 4, 10] and herein are of interest in themselves, but it is the authors' view that they serve another and higher purpose. The results of such studies tend to reinforce one's confidence in theories of macroscopic behavior founded on the averaging theorem and the kinematic mechanisms of lattice straining and crystallographic slip. The essential elements of these theories at small strain are now established (in particular, see [11]) and significant progress at large deformations has recently been made. The interested reader is referred to a series of interconnected papers by Hill[33], Hill and Rice[34], and Havner[35], the last of which focuses upon large pressure effects and their bearing upon a precise normality rule.

Acknowledgement—Appreciation is expressed to the National Science Foundation, Solid Mechanics Program, for support of this research through Grant GK-31313.

REFERENCES

1. G. I. Taylor, Plastic strain in metals, *J. Inst. Metals* **62**, 307 (1938).
2. G. I. Taylor, Analysis of plastic strain in a cubic crystal, *Stephen Timoshenko 60th Anniversary Volume*, pp. 218–224. Macmillan, London (1938).
3. T. H. Lin, Physical theory of plasticity, *Advances in Applied Mechanics* Vol. 11, pp. 255–311. Academic Press, New York (1971).
4. J. W. Hutchinson, Elastic–plastic behaviour of polycrystalline metals and composites, *Proc. R. Soc., Lond.* **A319**, 247 (1970).
5. K. S. Havner, A discrete model for the prediction of subsequent yield surfaces in polycrystalline plasticity, *Int. J. Solids Struct.* **7**, 719 (1971).
6. A. V. Hershey, The plasticity of an isotropic aggregate of anisotropic face-centered cubic crystals, *J. appl. Mech.* **21**, 241 (1954).
7. R. Hill, Continuum micro-mechanics of elastoplastic polycrystals, *J. Mech. Phys. Solids* **13**, 89 (1965).
8. K. S. Havner, On convergence of a discrete aggregate model in polycrystalline plasticity, *Int. J. Solids Struct.* **7**, 1269 (1971).
9. K. S. Havner, An analytical model of large deformation effects in crystalline aggregates, *Foundations of Plasticity* (Warsaw Symposium, 1972) (edited by A. Sawczuk), pp. 93–106. Noordhoff, Amsterdam.
10. K. S. Havner and R. Varadarajan, A quantitative study of a crystalline aggregate model, *Int. J. Solids Structures* **9**, 379 (1973).
11. R. Hill, The essential structure of constitutive laws for metal composites and polycrystals, *J. Mech. Phys. Solids* **15**, 79 (1967).
12. R. Hill, The mechanics of quasi-static plastic deformation in metals, *Surveys in Mechanics* (*G. I. Taylor 70th Anniversary Volume*) (edited by G. K. Batchelor and R. M. Davies), pp. 7–31. Cambridge University Press, London (1956).
13. T. H. Lin, Microstress fields of slip bands and inhomogeneity of plastic deformation of metals, *Foundations of Plasticity* (Warsaw Symposium, 1972) (edited by A. Sawczuk), pp. 77–91. Noordhoff, Amsterdam.
14. J. Mandel, Generalization de la theorie de plasticite de W. T. Koiter, *Int. J. Solids Struct.* **1**, 273 (1965).
15. R. Hill, Generalized constitutive relations for incremental deformation of metal crystals by multislip, *J. Mech. Phys. Solids* **14**, 95 (1966).
16. W. M. Mair and H. LL.D. Pugh, Effect of pre-strain on yield surfaces in copper, *J. mech. Engng. Sci.* **6**, 150 (1964).
17. M. Ronay, Second-order elongation of metal tubes in cyclic torsion, *Int. J. Solids Struct.* **4**, 509 (1968).
18. R. Hill, Elastic properties of reinforced solids: some theoretical principles, *J. Mech. Phys. Solids* **11**, 357 (1963).
19. J. F. W. Bishop and R. Hill, A theory of the plastic distortion of a polycrystalline aggregate under combined stresses, *Phil. Mag.* **42** (7), 414 (1951).
20. R. Hill, On macroscopic measures of plastic work and deformation in microheterogeneous media, *Prik. Mat. Mekh.* **35**, 31 (1971).
21. W. Prager, Recent developments in the mathematical theory of plasticity, *J. appl. Phys.* **20**, 235 (1949).

22. D. C. Drucker, A more fundamental approach to plastic stress–strain relations, *Proc. 1st U.S. natn. Congr. appl. Mech.*, pp. 487–491 (1951).
23. R. Hill, *The Mathematical Theory of Plasticity*, Chap. III. Oxford University Press, London (1950).
24. H. P. Künzi and W. Krelle, *Nonlinear Programming*, Chap. 5. Blaisdell, New York (1966).
25. J. F. Nye, *Physical Properties of Crystals*, Chap. 8. Oxford University Press, London (1957).
26. G. I. Taylor, The distortion of aluminum crystals under compression—II, *Proc. R. Soc., Lond.* **A116**, 16 (1927).
27. R. Von Mises, Mechanik der plastischen formänderung von kristallen, *Z. angew. Math. Mech.* **8**, 161 (1928).
28. W. S. Farren and G. I. Taylor, The heat developed during plastic extension of metals. *Proc. R. Soc., Lond.* **A107**, 422 (1925).
29. G. I. Taylor and H. Quinney, The latent energy remaining in a metal after cold working, *Proc. R. Soc., Lond.* **A143**, 307 (1934).
30. H. Quinney and G. I. Taylor, The emission of the latent energy due to previous cold working when a metal is heated, *Proc. R. Soc., Lond.* **A163**, 157 (1937).
31. O. W. Dillon, Jr., Plastic deformation waves and heat generated near the yield point of annealed aluminum, *Mechanical Behavior of Materials under Dynamic Loads* (edited by U. S. Lindholm), pp. 21–60 Springer, Berlin (1968).
32. T. H. Lin and M. Ito, Latent elastic strain energy due to the residual stresses in a plastically deformed polycrystal, *J. appl. Mech.* **34**, 606 (1967).
33. R. Hill, On constitutive macro-variables for heterogeneous solids at finite strain, *Proc. R. Soc., Lond.* **A326**, 131 (1972).
34. R. Hill and J. R. Rice, Constitutive analysis of elastic-plastic crystals at arbitrary strain, *J. Mech. Phys. Solids* **20**, 401 (1972).
35. K. S. Havner, On the mechanics of crystalline solids. *J. Mech. Phys. Solids*, **21**, 383 (1973).

Резюме — Рассчитывают значение величины нагружения при деформации почти одноосной модели алюминиевого кристаллического агрегата. Исследуют развитие кристаллографического скольжения; гистерезисный эффект в цикле напряжения; развитие генерирующегося тепла и скрытой энергии напряжения, образующихся во время пластической деформации. Между рассчитанными и экспериментальными результатами в отношении процентов тепла и скрытой энергии нашли удовлетворительное соответствие. Включают доказательство, что общая рассеянная механическая энергия на много менее, чем макроскопическая работа пластической деформации всего пробега частиц.